HHS Public Access

Author manuscript

Biochem J. Author manuscript; available in PMC 2015 April 01.

Published in final edited form as:

Biochem J. 2014 July 1; 461(1): 137–146. doi:10.1042/BJ20131438.

Drp1 stabilizes p53 on the mitochondria to trigger necrosis under oxidative stress conditions *in vitro* and *in vivo*

Xing Guo[*], **Hiromi Sesaki**[†], and **Xin Qi**[*,‡,1]

[*]Department of Physiology and Biophysics, Case Western Reserve University School of Medicine, 10900 Euclid Avenue, Cleveland, OH 44106, U.S.A.

[†]Department of Cell Biology, Johns Hopkins University School of Medicine, Baltimore, MD 21205, U.S.A.

[‡]Center for Mitochondrial Diseases, Case Western Reserve University School of Medicine, 10900 Euclid Avenue, Cleveland, OH 44106, U.S.A.

Abstract

Oxidative-stress-induced necrosis is considered to be one of the main pathological mediators in various neurological disorders, such as brain ischaemia. However, little is known about the mechanism by which cells modulate necrosis in response to oxidative stress. In the present study, we showed that Drp1 (dynamin-related protein 1), a primary mitochondrial fission protein, stabilizes the well-known stress gene p53 and is required for p53 translocation to the mitochondria under conditions of oxidative stress. We found that Drp1 binding to p53 induced mitochondria-related necrosis. In contrast, inhibition of Drp1 hyperactivation by Drp1 siRNA reduced necrotic cell death in cell cultures exposed to oxidative stress. Most significantly, we demonstrated that inhibition of Drp1 by the Drp1 peptide inhibitor P110, which was developed recently by our group, abolished p53 association with the mitochondria and reduced brain infarction in rats subjected to brain ischaemia/reperfusion injury. Taken together, these findings reveal a novel mechanism of Drp1 hyperactivation in the induction of mitochondrial damage and subsequent cell death. We propose that a Drp1 inhibitor such as P110 is a possible therapeutic agent for diseases in which hyperactivated Drp1 contributes to the pathology.

Keywords

dynamin-related protein 1 (Drp1); mitochondrion; necrosis; oxidative stress; p53; ubiquitination

INTRODUCTION

Mitochondria are critical subcellular organelles that govern energy generation, lipid metabolism and Ca^{2+} buffering. A decline in mitochondrial activity has been implicated in a

[1]To whom correspondence should be addressed (xxq38@case.edu).

AUTHOR CONTRIBUTION

Xing Guo performed most of the experiments. Hiromi Sesaki provided $Drp1^{WT}$ and $Drp1^{KO}$ MEFs, advised on confocal imaging analysis and revised the paper. Xin Qi designed and supervised the study and wrote the paper.

number of cellular processes, linking dysfunctional mitochondria to the pathogenesis of a wide range of human diseases, including neurological, cardiovascular and metabolic disorders [1–4].

Drp1 (dynamin-related protein 1) is a large GTPase that controls the process of mitochondrial division [3,5]. Drp1 localizes mainly to the cytoplasm. Upon activation, Drp1 translocates to the mitochondria where it binds to its mitochondrial adaptors, such as Fis1, Mff and MiD49/51, to process fission [6–8]. Mice lacking Drp1 exhibit embryo lethality [9]. Brain-specific conditional knockout of Drp1 in mice results in synaptic formation defects [10]. These lines of evidence suggest that Drp1 is required for normal brain development. In contrast, Drp1-mediated excessive mitochondrial fission was reported to play a causal role in apoptosis and autophagy-associated cell death [11–14]. More recently, Drp1 hyperactivation was demonstrated to participate in TNFα (tumour necrosis factor α)-induced mitochondrial signalling, initiating an early step in necrosis execution [15]. Notably, inhibition of Drp1 by either a dominant mutant $Drp1^{K38A}$ or RNAi reduces mitochondrial damage and increases cell survival in cells exposed to a variety of stimuli [13–15]. Therefore hyperactivated Drp1-induced mitochondrial dysfunction may represent a convergence of PCD (programmed cell death) pathways.

Tumour suppressor p53 is a transcriptional factor that mediates cell death through transcription-dependent and -independent pathways [16–19]. Under physiological conditions, p53 is maintained at a low level primarily by the oncoprotein MDM2 (mouse double minute 2 homologue), a p53 ubiquitin E3 ligase. MDM2 binds to p53, promoting p53 ubiquitination and degradation through the proteasome system [20]. However, upon cell stress, a cytoplasmic pool of p53 mainly translocates to the mitochondria, an event that precedes its transcriptional activity [16,19–21]. Mitochondrially targeted p53 has been shown to launch apoptosis by activating pro-apoptotic members of the Bcl-2 family at the mitochondrial outer membrane [16]. It is also reported that p53 enters the mitochondrial matrix where it binds to and inactivates MnSOD1 (manganese superoxide dismutase 1) to induce oxidative stress [22]. Furthermore, p53 accumulation on the mitochondria results in the opening of the mitochondrial permeability transition pore and subsequent necrosis by interacting with the mitochondrial inner membrane protein CypD (cyclophilin D) [18]. Taken together, these findings emphasize that translocation of p53 to the mitochondria leads to mitochondria-related cell death. However, the mechanism through which p53 is translocated to the mitochondria remains unclear.

In the present study, we have demonstrated that Drp1 stabilized p53 and was required for p53 translocation to the mitochondria under oxidative stress. We have shown that Drp1 binding to p53 induced mitochondria-associated necrosis in cultured cells exposed to oxidative stress. We also provided evidence that pharmacological inhibition of Drp1 hyperactivation is sufficient to reduce necrosis induced by brain ischaemic injury in rats.

EXPERIMENTAL

Antibodies and reagents

Cycloheximide, 3-NP (3-nitropropionic acid), etoposide and protease inhibitor cocktail were purchased from Sigma–Aldrich. MG132 was from Tocris Bioscience. Antibodies against c-Myc, FLAG, GFP, HA (haemagglutinin), p53, ubiquitin and HSP60 (heat-shock protein 60) were from Santa Cruz Biotechnology, and anti-Drp1 (DLP1) was from BD Biosciences. Anti-PARP [poly(ADP-ribose) polymerase] antibody was purchased from Cell Signaling Technology. Anti-VDAC (voltage-dependent anion channel) and anti-(cytochrome *c*) antibodies were from MitoScience, and anti-pan-actin antibody was from Sigma–Aldrich. Anti-Bax and anti-HMGB1 (high-mobility group box B1) antibodies were from Proteintech. Anti-(mouse IgG) and horseradish-peroxidase-linked species-specific antibodies were from Thermo Scientific and Abcam (only recognizing the light chain).

Constructs and transfection

Full-length Drp1, FLAG–p53, GFP–p53, HA–ubiquitin (wild-type), HA–Ub K0 (ubiquitin lacking lysine residues), HA–ubiquitin (Lys^{48}-linked) and ubiquitin (Lys^{63}-linked) plasmids were obtained from Addgene. Truncating mutations of Drp1 were created by inserting PCR-amplified fragments into the pCMV-Myc vector. Myc–p53 truncated mutants were gifts from Dr Lingqiang Zhang (Beijing Institute of Radiation Medicine, Beijing, China).

Cell culture

$Drp1^{WT}$ (wild-type Drp1) and $Drp1^{KO}$ (Drp1-knockout) MEFs (mouse embryonic fibroblasts) were gifts from Dr Hiromi Sesaki (Johns Hopkins University). Human breast cancer MCF7 cells and Drp1 MEFs were maintained in DMEM (Dulbecco's modified Eagle's medium) supplemented with 10% (v/v) heat-inactivated FBS and 1% (v/v) penicillin/streptomycin. Human non-small-cell lung cancer p53-null H1299 cells were maintained in RPMI 1640 medium with 10% (v/v) FBS and 1% (v/v) penicillin/streptomycin. All of the above-mentioned cells were maintained at 37°C in 5% CO_2/95% air.

Isolation of mitochondria-enriched fraction and lysate preparation

Cells were washed with ice-cold PBS and incubated on ice in lysis buffer (250 mM sucrose, 20 mM Hepes/NaOH, pH 7.5, 10 mM KCl, 1.5 mM $MgCl_2$, 1 mM EDTA, 1:300 dilution protease inhibitor cocktail and 1:300 dilution phosphatase inhibitor cocktail) for 30 min. Cells were then scraped and disrupted by repeated aspiration through a 25-gauge needle. Brain tissue was minced and ground using a pestle in lysis buffer. The homogenates were spun at 800 ***g*** for 10 min at 4°C, and the resulting supernatants were spun at 10000 ***g*** for 20 min at 4°C. The pellets were washed with lysis buffer and spun at 10000 ***g*** again for 20 min at 4°C. The final pellets were suspended in lysis buffer containing 1% (v/v) Triton X-100 and were mitochondria-enriched fractions. Mitochondrial membrane protein VDAC or HSP60 was used as a loading control.

Immunoprecipitation

Cells were lysed in total cell lysate buffer [50 mM Tris/HCl, pH 7.5, containing 150 mM NaCl, 1% (v/v) Triton X-100 and protease inhibitor]. Soluble protein was incubated with indicated antibody overnight at 4°C and Protein A/G–beads for 1 h. Immunoprecipitates were washed four times with cell lysate buffer, analysed by SDS/PAGE and immunoblotted with the indicated antibodies.

Measurement of MMP (mitochondrial membrane potential) and mitochondrial superoxide production

Cells cultured on coverslips were washed with ice-cold PBS and then incubated with 5 μM MitoSOX™ Red (Invitrogen), a mitochondrial superoxide indicator, for 10 min at 37°C. To measure the MMP in cultures, the cells were incubated with 10 μM TMRM (tetramethylrhodamine) (Invitrogen) for 20 min at 37°C. The cells were then washed with PBS and mounted. The images were visualized by microscope, and quantification of images was then carried out using NIH ImageJ software. At least 100 cells per group were counted in the analysis.

Immunocytochemistry

Cells cultured on coverslips were washed with ice-cold PBS, fixed in 4% (w/v) formaldehyde and permeabilized with 0.1% Triton X-100. After incubation with 2% (v/v) normal goat serum (to block non-specific staining), fixed cells were incubated overnight at 4 °C with antibodies against p53 (1:2000 dilution, Cell Signaling Biotechnology) and Tom20 (translocase of the outer membrane 20) (1:500 dilution, Santa Cruz Biotechnology). Cells were washed with PBS and incubated with Alexa Fluor® 488-conjugated anti-rabbit and Alexa Fluor® 568-conjugated anti-mouse secondary antibodies (1:500 dilution, Invitrogen) for 60 min. Coverslips were mounted on glass slides and imaged by confocal fluorescence microscopy using an inverted Olympus IX-81 coupled Fluoview 1000 (FV 1000) confocal microscope.

Determination of total ATP levels

Cellular ATP concentration was measured using an ATP Colorimetric/Fluorometric Assay Kit (BioVision). The cells were lysed in 50 μl of ATP assay buffer, and total ATP levels were determined at 570 nm using a microplate reader, according to the manufacturer's instructions.

HMGB1 release assay

Medium from cultured cells was harvested. Proteins in medium were purified using Amicon Ultra 0.5 ml centrifugal filters (Millipore) and analysed by Western blotting with anti-HMGB1 antibody.

MCAO (middle cerebral artery occlusion) stroke model

Transient cerebral ischaemia was induced in male Sprague–Dawley rats (250–280 g) using an occluding intraluminal suture, as described previously [23,24]. Briefly, an uncoated 30-mm-long segment of 3-0 nylon monofilament suture with the tip rounded by a flame was

inserted into the stump of the external carotid artery and advanced into the internal carotid artery ~19–20 mm from the bifurcation to occlude the ostium of the middle cerebral artery. At the end of the ischaemic period (2 h), the suture was removed and the animal was allowed to recover. Animals were maintained under isoflurane anaesthesia during all surgical procedures. Physiological parameters including body temperature (35–38°C) and respiration rate were monitored and maintained using a heat blanket and anaesthetic adjustment. Control peptide carrier Tat (transactivator of transcription) or Drp1 peptide inhibitor P110 was delivered as an i.p. (intraperitoneal) dose (0.5 mg/kg of body weight). Brain infarction size was measured by staining coronal brain slices (2 mm/slice) with 2% (w/v) TTC (triphenyltetrazolium chloride), and the neurological status of the rats was evaluated by an observer blinded to the treatment groups, using the methods described previously [23,25]. The procedures involving animals in the present study were performed in accordance with the National Institutes of Health Guide for the Care and Use of Laboratory Animals and with protocols approved by the Institutional Animal Care and Use Committee of Case Western Reserve University. These protocols include efforts to minimize animal suffering and the number of rats used.

Western blot analysis

Protein concentrations were determined using the Bradford assay. Proteins were resuspended in Laemmli buffer, loaded on SDS/PAGE and transferred on to nitrocellulose membranes. Membranes were probed with the indicated antibody and then visualized by ECL.

Statistical methods

Data are expressed as means ±S.D. An unpaired Student's *t* test assessed differences between two groups; a one-factor ANOVA with Fisher's test was used to assess differences between more than two groups; and Fisher's test for categorical data was used to assess significance ($P < 0.05$). All experiments were performed at least three times independently.

RESULTS

Drp1 stabilizes p53

Recent studies have found that p53 participated in Drp1-mediated cell death in cardiomyocytes exposed to hydrogen peroxide (H_2O_2) [26] and in neuronal cells in response to DNA damage [27]. To determine the interdependence between Drp1 and p53, we first examined the protein level of p53 in $Drp1^{WT}$ and $Drp1^{KO}$ MEFs. In $Drp1^{KO}$ MEFs, we found a dramatic decrease in the p53 protein level, when compared with that in $Drp1^{WT}$ MEFs (Figure 1A). This decrease in the p53 protein level was not due to a down-regulation in the p53 mRNA level (Figure 1B), determined by RT (reverse transcription)–PCR using the primers listed in Supplementary Table S1 at http://www.biochemj.org/bj/461/bj4610137add.htm. In contrast, the addition of MG132, a proteasome inhibitor, recovered the protein level of p53 in $Drp1^{KO}$ MEFs (Figure 1A). These findings suggest that protein degradation causes a decrease in the p53 protein level. Complementation assays showed that overexpression of Myc–Drp1 led to an increase in the protein level of FLAG–p53 in both p53-null human lung cancer H1299 cells (Figure 1C) and human breast adenocarcinoma

MCF7 cells (Figure 1D, lower panel). Furthermore, a prolonged half-life of p53 was observed in Drp1^{WT} MEFs and MCF7 cells expressing Myc–Drp1, when compared with that in Drp1^{KO} MEFs and in MCF7 cells expressing a control vector respectively (Figure 1D). Collectively, the above data indicate that Drp1 stabilizes p53.

Drp1 is required for p53 accumulation on the mitochondria under oxidative stress

Drp1 translocation to the mitochondria initiates mitochondrial fission and, upon severe stress, induces mitochondrial dysfunction and cell death [3,28]. A directly detrimental effect of p53 at the mitochondria was also documented in various cell types exposed to genotoxic, hypoxic and oxidative stress [16,19–21]. Given that Drp1 stabilizes p53 (Figure 1), we next asked whether Drp1 affects p53 association with the mitochondria. In Drp1^{WT} MEFs exposed to H_2O_2 (an oxidative stress inducer) or 3-NP {a mitochondrial complex II inhibitor and an inducer of mitoROS (mitochondrial reactive oxygen species) [14]*}*, Western blot analysis of mitochondrial fractions showed a greater accumulation of p53 on the mitochondria, which was completely abolished in Drp1^{KO} MEFs (Figure 2A, left-hand and middle panels). Confocal microscopy analysis consistently revealed greater localization of p53 on the mitochondria in Drp1^{WT} MEFs exposed to either H_2O_2 or 3-NP than that in Drp1^{KO} MEFs (Figure 2B and 2C). In parallel, down-regulation of Drp1 by Drp1 siRNA in MCF-7 cells abrogated the accumulation of p53 on the mitochondria induced by H_2O_2 (Figure 2D). Furthermore, blocking Drp1 association with the mitochondria by the Drp1 peptide inhibitor P110, which was recently developed by our group [11,12,29], also abolished p53 levels on the mitochondria under the same conditions (Figure 2E). Interestingly, this event might be stress-specific because depletion of Drp1 did not block p53 translocation to the mitochondria when induced by etoposide, a DNA-damage inducer (Figure 2A, right-hand panel). Finally, complementation assay showed that expression of Myc–Drp1 induced FLAG–p53 accumulation on the mitochondria in MCF7 cells (Figure 2F). Taken together, these findings demonstrate that Drp1 is required for translocation of p53 to the mitochondria, especially under conditions of oxidative stress.

Drp1 interacts with p53

To examine whether Drp1 and p53 interact, we performed co-immunoprecipitation analysis. As shown in Figure 3(A) (upper panel), GFP–p53 was specifically immunoprecipitated with Myc–Drp1 by the anti-Myc antibody. An endogenous interaction between Drp1 and p53 was observed in Drp1^{WT} MEFs and MCF-7 cells using anti-Drp1 and anti-p53 antibodies (Figure 3A, lower panels). Here, we noticed a slight shift up on the band of Drp1 after immunoprecipitation, when compared with that in input. A number of previous studies, including ours, have shown that Drp1 can be post-translationally modified, such as by phosphorylation, ubiquitination and SUMOylation [11,30,31]. Thus it is possible that such a shift up is due to p53 binding to a post-translationally modified Drp1. However, the exact mechanism remains to be determined.

Using a series of truncated mutants, we mapped the p53 interaction site to the GTPase domain of Drp1 (amino acids 1–335) (Figure 3B). The Drp1-interaction site in p53 was mapped to the DBD (DNA-binding domain) of p53, amino acids 113–290 (Figure 3C). Next, we co-expressed the p53 deletion mutants with Myc–Drp1 in p53-null H1299 cells.

We found that Drp1-induced p53 association with the mitochondria was abolished in cells expressing the Myc–p53-M-D1 mutant, which lacks a DBD, when compared with that in cells expressing either the Myc–p53-N-D2 or -C-D1 deletion mutant (Figure 3D). However, expression of Drp1 did not affect the total protein level of Myc–p53-M-D1 (Supplementary Figure S1 at http://www.biochemj.org/bj/461/bj4610137add.htm). Collectively, these data demonstrate that Drp1 and p53 interact physically and that the DBD of p53 is required for Drp1-induced p53 accumulation on the mitochondria.

Drp1 induces MDM2-mediated p53 mono-ubiquitination

Mono-ubiquitination of p53 provides a trafficking signal that redirects it from a fate of degradation in unstressed cells to mitochondrial translocation and activation at an early stage of the stress response [20,32]. Next, we determined whether Drp1 regulates p53 mono-ubiquitination in cells. In order to determine mono-ubiquitination of p53, we co-expressed Myc-tagged p53 deletion mutants with a mutant ubiquitin (HA–Ub K0) in which all lysine residues in the ubiquitin were mutated to arginine [33]. Following the methods described in previous papers [20,34], we immunoprecipitated the cell lysates with anti-Myc antibodies followed by Western blot analysis with anti-Myc antibodies, in the presence or absence of Drp1 plasmid. As shown in Figure 4(A), expression of Drp1 induced p53 mono-ubiquitination in cells expressing p53-N-D2 and p53-C-D1 mutants, but not in cells with p53-M-D1 mutant (Figure 4A). Given that the DBD of p53 bound to Drp1 and was required for p53 accumulation on the mitochondria (Figure 3), the above data indicate that the DBD is critical for p53 ubiquitination in the presence of Drp1. Thus Drp1-mediated p53 mono-ubiquitination might be a driving force for p53 translocation to the mitochondria.

It is commonly accepted that Lys^{48}-linked polyubiquitin chains constitute a signal for protein degradation by the 26S proteasome [35]. Moreover, Lys^{63}-linked polyubiquitination functions in a variety of cellular processes, including stress responses [36] and signal transduction [37,38]. In the present study, we found that expression of Drp1 induced neither Lys^{48}-linked nor Lys^{63}-linked polyubiquitination of p53 (Supplementary Figure S2 at http://www.biochemj.org/bj/461/bj4610137add.htm). These results support further the above finding that Drp1 stabilizes p53 by specifically mediating its mono-ubiquitination.

MDM2 mediates p53 mono-ubiquitination and promotes p53 mitochondrial translocation via its enzymatic E3 ligase activity [17,20,32]. We next asked whether MDM2 is a potential E3 ligase involved in Drp1-induced p53 mono-ubiquitination. As shown in Figures 4(B) and 4(C), expression of Drp1 dramatically increased FLAG–p53 mono-ubiquitination in the presence of wild-type MDM2 (MDM2-WT) in p53-null H1299 cells. However, this Drp1-induced ubiquitination of p53 was abolished in cells expressing a MDM2 C464A mutant (MDM2-CA), which lacks E3 ligase activity (Figure 4B). These lines of evidence suggest that MDM2 might serve as an E3 ligase of p53 to mediate Drp1-induced p53 mono-ubiquitination.

Drp1 and p53 interdependently induce mitochondrial damage and trigger necrosis

Both Drp1 and p53 have been reported to direct mitochondrial death programmes, such as oxidative stress, apoptosis, necrosis and autophagy-associated cell death [3,16,39]. Next, we

determined whether p53 is implicated in Drp1 hyperactivation-induced mitochondrial damage. In p53-null H1299 cells, expression of p53 resulted in decreased MMP, increased mitoROS and reduced ATP levels (Figures 5A, 5C and 5D). These results agree with previous findings that p53 triggers mitochondrial dysfunction [16,17,19]. Importantly, co-expression of p53 and Drp1 led to more pronounced mitochondrial damage, as demonstrated by lower MMP and ATP as well as higher mitoROS than in cells expressing p53 alone (Figures 5A, 5C and 5D). An increase in cytochrome *c* release from mitochondria in cells expressing both Drp1 and p53 confirmed further a decrease in mitochondrial integrity (Figure 5B). Thus p53-induced mitochondrial damage was substantially enhanced by the presence of Drp1. We found that co-expression of Drp1 and p53 induced the release of HMGB1 and LDH (lactate dehydrogenase), both of which are classical biochemical hallmarks specific for necrotic cell death [40–42] (Figures 5E and 5F). However, expression of either Drp1 or p53 alone has no major effects on these events. These lines of evidence demonstrate that Drp1 and p53 interdependently enhance mitochondria-related necrosis. In parallel, in MCF-7 cells exposed to H_2O_2, down-regulation of Drp1 by Drp1 siRNA, which abolished p53 accumulation on the mitochondria (Figure 1), reduced the loss of MMP and the release of HMGB1 (Figures 5G and 5H). These findings underscore further the importance of Drp1 in oxidative stress-induced mitochondria-related necrosis.

Stress-induced accumulation of p53 on the mitochondria can trigger apoptotic cell death [17,43]. In the present study, we found that co-expression of Drp1 and p53 did not affect apoptotic markers, such as Bax translocation to the mitochondria [44] (Figure 5B) or cleavage of PARP [45] (Figure 5E). Moreover, p53 alone is not sufficient to induce the activity of apoptotic molecules (Figure 5E). Thus it is very likely that additional factors, upon activation, are required for p53-induced mitochondria-related apoptosis.

Inhibition of Drp1 hyperactivation reduced brain infarction in rats subjected to brain ischaemia/reperfusion

Next, we investigated the physiological importance of Drp1 in necrosis execution. Brain infarction, a classic example of necrosis, is characterized by mitochondrial dysfunction, enhanced generation of ROS (reactive oxygen species) and ATP depletion [46]. Thus we determined whether hyperactivated Drp1 plays a crucial role in brain infarction in rats subjected to brain ischaemia/reperfusion injury. Following a transient MCAO in rats, we observed increased association of both Drp1 and p53 with the mitochondria in the brain (Figures 6A and 6B). We then treated these rats with a peptide inhibitor of Drp1 mitochondrial translocation, P110, which we developed recently [11,12,29]. We found that both Drp1 and p53 association with the mitochondria were inhibited in rats treated with P110 (0.5 mg/kg of body weight, i.p. injection), when compared with those in vehicle-treated rats (Figure 6A and 6B). These data are consistent with our findings in culture and demonstrate that Drp1 is required for p53 mitochondrial localization *in vivo* under brain ischaemic conditions.

We found that 2 h of ischaemia followed by 24 h of reperfusion led to approximately 27% ATP reduction and 44% infarction, whereas treatment with P110 increased the ATP level by over 50% (Figure 6C) and reduced the infarction size from 44 to 13% (Figure 6E).

Moreover, the reduction of brain infarction by P110 treatment was associated with a better outcome of neurological status in rats (Figure 6D), a more clinically relevant endpoint of a treatment's effect. Taken together, the above data demonstrate that inhibition of Drp1 hyperactivation is sufficient to reduce brain infarction induced by brain ischaemia/reperfusion injury.

DISCUSSION

In the present study, we have identified two new steps in Drp1-induced mitochondrial damage and subsequent cell death: first, Drp1 stabilizes p53 and is required for p53 recruitment to the mitochondria under oxidative stress, and, secondly, Drp1 and p53 interdependently induce mitochondria-associated necrosis. Thus our findings represent a novel mechanism by which cells modulate necrosis in response to oxidative stress *in vitro* and *in vivo*.

Drp1 has been demonstrated to participate in PCD in response to different stimuli. Staurosporine and CD47 induce apoptosis by recruiting Drp1 to the mitochondria, leading to MMP loss and disruption of mitochondrial structure [47,48]. TNFα, ROS and Ca^{2+} ionophores induce Drp1 dephosphorylation at Ser^{637} via activation of PGAM5 (phosphoglycerate mutase family member 5), which causes mitochondria-related necrosis [15]. Nevertheless, the downstream signals of Drp1-induced mitochondria-related cell death remain unknown. In the present study, we found that, under oxidative stress, Drp1 was required for p53 translocation to the mitochondria where Drp1 and p53 interdependently enhanced the mitochondrial membrane depolarization and the mitochondrial superoxide production, and reduced ATP content. Moreover, this Drp1/p53-induced mitochondrial damage was associated with an increase in necrotic cell death markers, such as HMGB1 and LDH release, but had no effect on apoptotic markers. Furthermore, depletion of p53 abolished Drp1-induced mitochondrial damage and necrotic cell death. Thus these lines of evidence indicate that Drp1-induced mitochondrial damage and cell death might be under the control of p53.

Under physiological conditions, the half-life of p53 ranges from 6 to 20 min, an observation that has long been reported. However, upon stress, p53 is stabilized in the cytoplasm by various factors and initiates the subsequent cell death programme. p53 does not contain an MLS (mitochondrial localization signal), and its mitochondrial translocation does not result from post-translation acetylation and phosphorylation [16]. Rather, it appears that MDM2-mediated mono-ubiquitination is the major driving force of p53 translocation to the mitochondria [17,19,20]. In the present study, Drp1 is most likely to induce MDM2-dependent monoubiquitination of p53 in the cytosol, which in turn leads to p53 translocation to the mitochondria. Such a speculation is also supported by the finding that Drp1 induced neither Lys^{48}- nor Lys^{63}-linked poly-ubiquitination of p53 (Supplementary Figure S2). However, it remains to be determined whether Drp1 directly or indirectly affects MDM2, which leads to p53 monoubiquitination. In addition to MDM2, the E3 ubiquitin ligase MSL2 (male-specific lethal 2-like) has been shown to control cytoplasmic localization of p53 (but not its stability) in an MDM2-independent fashion [20,32]. Thus the possibility that Drp1-induced p53 mono-ubiquitination involves other E3 ligases remains to be determined.

It is generally accepted that mitochondrial dysfunction is a critical part of the necrotic process, with a collapse in MMP resulting in excessive ROS production and a lack of ATP production [49]. One suggested mechanism for mitochondria-associated necrotic cell death is CypD-dependent mitochondrial permeability transition pore opening under oxidative stress, which leads to mitochondrial swelling, energy failure and increased ROS levels [50,51]. Interestingly, a recent study found that, upon oxidative stress, translocation of p53 to the mitochondria triggered mitochondrial permeability transition pore opening by engaging in a physical interaction with CypD, which induced necrotic cell death [18]. Thus our finding that p53 requires Drp1 to initiate the mitochondrial necrotic pathway deepens the understanding of the p53 necrotic machinery. Previous studies reported that blocking p53 association with the mitochondria by cyclosporin [18] or pifithrin-μ [52] greatly reduced tissue necrosis in rodents subjected to ischaemic injury. In the present study, we found that P110 treatment-induced inhibition of Drp1 association with the mitochondria inhibited p53 accumulation on the mitochondria and reduced infarction size. In combination with the results in cultured cells, our findings indicate that inhibition of Drp1 hyperactivation is sufficient to reduce tissue damage caused by ischaemic reperfusion injury. Thus we propose that a Drp1 peptide inhibitor, such as a P110-like compound, might be useful in the treatment of ischaemic injury, such as stroke.

Supplementary Material

Refer to Web version on PubMed Central for supplementary material.

Acknowledgments

FUNDING

This work is supported by a American Heart Association (AHA) Beginning Grant-In-Aid [grant number 12BGIA8800014 (to X.Q.)] and the National Institutes of Health [R01 grant numbers NS088192 (to X. Q.) and GM089853 (to H.S.)].

Abbreviations

CypD	cyclophilin D
DBD	DNA-binding domain
Drp1	dynamin-related protein 1
Drp1^{KO}	Drp1-knockout
Drp1^{WT}	wild-type Drp1
HA	haemagglutinin
HMGB1	high-mobility group box B1
HSP60	heat-shock protein 60
i.p.	intraperitoneal
LDH	lactate dehydrogenase

MCAO	middle cerebral artery occlusion
MDM2	mouse double minute 2 homologue
MEF	mouse embryonic fibroblast
mitoROS	mitochondrial reactive oxygen species
MMP	mitochondrial membrane potential
3-NP	3-nitropropionic acid
PARP	poly(ADP-ribose) polymerase
PCD	programmed cell death
ROS	reactive oxygen species
Tat	transactivator of transcription
TNFα	tumour necrosis factor α
Tom20	translocase of the outer membrane 20
Ub K0	ubiquitin lacking lysine residues
VDAC	voltage-dependent anion channel

REFERENCES

1. Beal MF. Mitochondria take center stage in aging and neurodegeneration. Ann. Neurol. 2005; 58:495–505. CrossRef PubMed. [PubMed: 16178023]
2. DiMauro S, Schon EA. Mitochondrial disorders in the nervous system. Annu. Rev. Neurosci. 2008; 31:91–123. CrossRef PubMed. [PubMed: 18333761]
3. Su Y, Qi X. Impairment of mitochondrial dynamics: a target for the treatment of neurological disorders? Future Neurol. 2013; 8:333–346. CrossRef.
4. Gustafsson AB, Gottlieb RA. Heart mitochondria: gates of life and death. Cardiovasc. Res. 2008; 77:334–343. CrossRef PubMed. [PubMed: 18006487]
5. Chan DC. Mitochondria: dynamic organelles in disease, aging, and development. Cell. 2006; 125:1241–1252. CrossRef PubMed. [PubMed: 16814712]
6. James DI, Parone PA, Mattenberger Y, Martinou JC. hFis1, a novel component of the mammalian mitochondrial fission machinery. J. Biol. Chem. 2003; 278:36373–36379. CrossRef PubMed. [PubMed: 12783892]
7. Palmer CS, Osellame LD, Laine D, Koutsopoulos OS, Frazier AE, Ryan MT. MiD49 and MiD51, new components of the mitochondrial fission machinery. EMBO Rep. 2011; 12:565–573. CrossRef PubMed. [PubMed: 21508961]
8. Otera H, Wang C, Cleland MM, Setoguchi K, Yokota S, Youle RJ, Mihara K. Mff is an essential factor for mitochondrial recruitment of Drp1 during mitochondrial fission in mammalian cells. J. Cell. Biol. 2010; 191:1141–1158. CrossRef PubMed. [PubMed: 21149567]
9. Ishihara N, Nomura M, Jofuku A, Kato H, Suzuki SO, Masuda K, Otera H, Nakanishi Y, Nonaka I, Goto Y, et al. Mitochondrial fission factor Drp1 is essential for embryonic development and synapse formation in mice. Nat. Cell Biol. 2009; 11:958–966. CrossRef PubMed. [PubMed: 19578372]
10. Wakabayashi J, Zhang Z, Wakabayashi N, Tamura Y, Fukaya M, Kensler TW, Iijima M, Sesaki H. The dynamin-related GTPase Drp1 is required for embryonic and brain development in mice. J. Cell Biol. 2009; 186:805–816. CrossRef PubMed. [PubMed: 19752021]

11. Su YC, Qi X. Inhibition of excessive mitochondrial fission reduced aberrant autophagy and neuronal damage caused by LRRK2 G2019S mutation. Hum. Mol. Genet. 2013; 22:4545–4561. CrossRef PubMed. [PubMed: 23813973]
12. Qi X, Qvit N, Su YC, Mochly-Rosen D. A novel Drp1 inhibitor diminishes aberrant mitochondrial fission and neurotoxicity. J. Cell Sci. 2013; 126:789–802. CrossRef PubMed. [PubMed: 23239023]
13. Frank S, Gaume B, Bergmann-Leitner ES, Leitner WW, Robert EG, Catez F, Smith CL, Youle RJ. The role of dynamin-related protein 1, a mediator of mitochondrial fission, in apoptosis. Dev. Cell. 2001; 1:515–525. CrossRef PubMed. [PubMed: 11703942]
14. Liot G, Bossy B, Lubitz S, Kushnareva Y, Sejbuk N, Bossy-Wetzel E. Complex II inhibition by 3-NP causes mitochondrial fragmentation and neuronal cell death via an NMDA- and ROS-dependent pathway. Cell Death Differ. 2009; 16:899–909. CrossRef PubMed. [PubMed: 19300456]
15. Wang Z, Jiang H, Chen S, Du F, Wang X. The mitochondrial phosphatase PGAM5 functions at the convergence point of multiple necrotic death pathways. Cell. 2012; 148:228–243. CrossRef PubMed. [PubMed: 22265414]
16. Galluzzi L, Morselli E, Kepp O, Vitale I, Pinti M, Kroemer G. Mitochondrial liaisons of p53. Antioxid. Redox Signal. 2011; 15:1691–1714. CrossRef PubMed. [PubMed: 20712408]
17. Marchenko ND, Zaika A, Moll UM. Death signal-induced localization of p53 protein to mitochondria: a potential role in apoptotic signaling. J. Biol. Chem. 2000; 275:16202–16212. CrossRef PubMed. [PubMed: 10821866]
18. Vaseva AV, Marchenko ND, Ji K, Tsirka SE, Holzmann S, Moll UM. p53 opens the mitochondrial permeability transition pore to trigger necrosis. Cell. 2012; 149:1536–1548. CrossRef PubMed. [PubMed: 22726440]
19. Vaseva AV, Moll UM. The mitochondrial p53 pathway. Biochim. Biophys. Acta. 2009; 1787:414–420. CrossRef PubMed. [PubMed: 19007744]
20. Marchenko ND, Wolff S, Erster S, Becker K, Moll UM. Monoubiquitylation promotes mitochondrial p53 translocation. EMBO J. 2007; 26:923–934. CrossRef PubMed. [PubMed: 17268548]
21. Zhao Y, Chaiswing L, Velez JM, Batinic-Haberle I, Colburn NH, Oberley TD, St Clair DK. p53 translocation to mitochondria precedes its nuclear translocation and targets mitochondrial oxidative defense protein-manganese superoxide dismutase. Cancer Res. 2005; 65:3745–3750. CrossRef PubMed. [PubMed: 15867370]
22. Pani G, Galeotti T. Role of MnSOD and p66shc in mitochondrial response to p53. Antioxid. Redox Signal. 2011; 15:1715–1727. CrossRef PubMed. [PubMed: 20712406]
23. Bright R, Raval AP, Dembner JM, Perez-Pinzon MA, Steinberg GK, Yenari MA, Mochly-Rosen D. Protein kinase Cδ mediates cerebral reperfusion injury *in vivo* . J. Neurosci. 2004; 24:6880–6888. CrossRef PubMed. [PubMed: 15295022]
24. Qi X, Mochly-Rosen D. The PKCδ-Abl complex communicates ER stress to the mitochondria: an essential step in subsequent apoptosis. J. Cell Sci. 2008; 121:804–813. CrossRef PubMed. [PubMed: 18285444]
25. Qi X, Hosoi T, Okuma Y, Kaneko M, Nomura Y. Sodium 4-phenylbutyrate protects against cerebral ischemic injury. Mol. Pharmacol. 2004; 66:899–908. CrossRef PubMed. [PubMed: 15226415]
26. Li J, Donath S, Li Y, Qin D, Prabhakar BS, Li P. miR-30 regulates mitochondrial fission through targeting p53 and the dynamin-related protein-1 pathway. PLoS Genet. 2010; 6:e1000795. CrossRef PubMed. [PubMed: 20062521]
27. Wang DB, Garden GA, Kinoshita C, Wyles C, Babazadeh N, Sopher B, Kinoshita Y, Morrison RS. Declines in *drp1* and *parkin* expression underlie DNA damage-induced changes in mitochondrial length and neuronal death. J. Neurosci. 2013; 33:1357–1365. CrossRef PubMed. [PubMed: 23345212]
28. Oettinghaus B, Licci M, Scorrano L, Frank S. Less than perfect divorces: dysregulated mitochondrial fission and neurodegeneration. Acta Neuropathol. 2012; 123:189–203. CrossRef PubMed. [PubMed: 22179580]

29. Guo X, Disatnik MH, Monbureau M, Shamloo M, Mochly-Rosen D, Qi X. Inhibition of mitochondrial fragmentation diminishes Huntington's disease-associated neurodegeneration. J. Clin. Invest. 2013; 123:5371–5388. CrossRef PubMed. [PubMed: 24231356]
30. Chang CR, Blackstone C. Dynamic regulation of mitochondrial fission through modification of the dynamin-related protein Drp1. Ann. N.Y. Acad. Sci. 2010; 1201:34–39. CrossRef PubMed. [PubMed: 20649536]
31. Santel A, Frank S. Shaping mitochondria: the complex posttranslational regulation of the mitochondrial fission protein DRP1. IUBMB Life. 2008; 60:448–455. CrossRef PubMed. [PubMed: 18465792]
32. Marchenko ND, Moll UM. The role of ubiquitination in the direct mitochondrial death program of p53. Cell Cycle. 2007; 6:1718–1723. CrossRef PubMed. [PubMed: 17630506]
33. Lim KL, Chew KC, Tan JM, Wang C, Chung KK, Zhang Y, Tanaka Y, Smith W, Engelender S, Ross CA, et al. Parkin mediates nonclassical, proteasomal-independent ubiquitination of synphilin-1: implications for Lewy body formation. J. Neurosci. 2005; 25:2002–2009. CrossRef PubMed. [PubMed: 15728840]
34. Muscolini M, Montagni E, Palermo V, Di Agostino S, Gu W, Abdelmoula-Souissi S, Mazzoni C, Blandino G, Tuosto L. The cancer-associated K351N mutation affects the ubiquitination and the translocation to mitochondria of p53 protein. J. Biol. Chem. 2011; 286:39693–39702. CrossRef PubMed. [PubMed: 21953469]
35. Thrower JS, Hoffman L, Rechsteiner M, Pickart CM. Recognition of the polyubiquitin proteolytic signal. EMBO J. 2000; 19:94–102. CrossRef PubMed. [PubMed: 10619848]
36. Arnason T, Ellison MJ. Stress resistance in *Saccharomyces cerevisiae* is strongly correlated with assembly of a novel type of multiubiquitin chain. Mol. Cell. Biol. 1994; 14:7876–7883. PubMed. [PubMed: 7969127]
37. Sun L, Chen ZJ. The novel functions of ubiquitination in signaling. Curr. Opin. Cell Biol. 2004; 16:119–126. CrossRef PubMed.
38. Mukhopadhyay D, Riezman H. Proteasome-independent functions of ubiquitin in endocytosis and signaling. Science. 2007; 315:201–205. CrossRef PubMed. [PubMed: 17218518]
39. Cho DH, Nakamura T, Lipton SA. Mitochondrial dynamics in cell death and neurodegeneration. Cell. Mol. Life Sci. 2010; 67:3435–3447. CrossRef PubMed. [PubMed: 20577776]
40. Bianchi ME, Manfredi A. Chromatin and cell death. Biochim. Biophys. Acta. 2004; 1677:181–186. CrossRef PubMed. [PubMed: 15020058]
41. Rovere-Querini P, Capobianco A, Scaffidi P, Valentinis B, Catalanotti F, Giazzon M, Dumitriu IE, Muller S, Iannacone M, Traversari C, et al. HMGB1 is an endogenous immune adjuvant released by necrotic cells. EMBO Rep. 2004; 5:825–830. CrossRef PubMed. [PubMed: 15272298]
42. Chen CF, Wang D, Hwang CP, Liu HW, Wei J, Lee RP, Chen HI. The protective effect of niacinamide on ischemia-reperfusion-induced liver injury. J. Biomed. Sci. 2001; 8:446–452. CrossRef PubMed. [PubMed: 11702007]
43. Leu JI, Dumont P, Hafey M, Murphy ME, George DL. Mitochondrial p53 activates Bak and causes disruption of a Bak-Mcl1 complex. Nat. Cell Biol. 2004; 6:443–450. CrossRef PubMed. [PubMed: 15077116]
44. Oltvai ZN, Milliman CL, Korsmeyer SJ. Bcl-2 heterodimerizes *in vivo* with a conserved homolog, Bax, that accelerates programmed cell death. Cell. 1993; 74:609–619. CrossRef PubMed. [PubMed: 8358790]
45. Lazebnik YA, Kaufmann SH, Desnoyers S, Poirier GG, Earnshaw WC. Cleavage of poly(ADP-ribose) polymerase by a proteinase with properties like ICE. Nature. 1994; 371:346–347. CrossRef PubMed. [PubMed: 8090205]
46. Golstein P, Kroemer G. Cell death by necrosis: towards a molecular definition. Trends Biochem. Sci. 2007; 32:37–43. CrossRef PubMed. [PubMed: 17141506]
47. Wasiak S, Zunino R, McBride HM. Bax/Bak promote sumoylation of DRP1 and its stable association with mitochondria during apoptotic cell death. J. Cell Biol. 2007; 177:439–450. CrossRef PubMed. [PubMed: 17470634]

48. Bras M, Yuste VJ, Roue G, Barbier S, Sancho P, Virely C, Rubio M, Baudet S, Esquerda JE, Merle-Beral H, et al. Drp1 mediates caspase-independent type III cell death in normal and leukemic cells. Mol. Cell. Biol. 2007; 27:7073–7088. CrossRef PubMed. [PubMed: 17682056]

49. Lemasters JJ, Nieminen AL, Qian T, Trost LC, Herman B. The mitochondrial permeability transition in toxic, hypoxic and reperfusion injury. Mol. Cell. Biochem. 1997; 174:159–165. CrossRef PubMed. [PubMed: 9309681]

50. Baines CP, Kaiser RA, Purcell NH, Blair NS, Osinska H, Hambleton MA, Brunskill EW, Sayen MR, Gottlieb RA, Dorn GW, et al. Loss of cyclophilin D reveals a critical role for mitochondrial permeability transition in cell death. Nature. 2005; 434:658–662. CrossRef PubMed. [PubMed: 15800627]

51. Nakagawa T, Shimizu S, Watanabe T, Yamaguchi O, Otsu K, Yamagata H, Inohara H, Kubo T, Tsujimoto Y. Cyclophilin D-dependent mitochondrial permeability transition regulates some necrotic but not apoptotic cell death. Nature. 2005; 434:652–658. CrossRef PubMed. [PubMed: 15800626]

52. Nijboer CH, Heijnen CJ, van der Kooij MA, Zijlstra J, van Velthoven CT, Culmsee C, van Bel F, Hagberg H, Kavelaars A. Targeting the p53 pathway to protect the neonatal ischemic brain. Ann. Neurol. 2011; 70:255–264. CrossRef PubMed. [PubMed: 21674585]

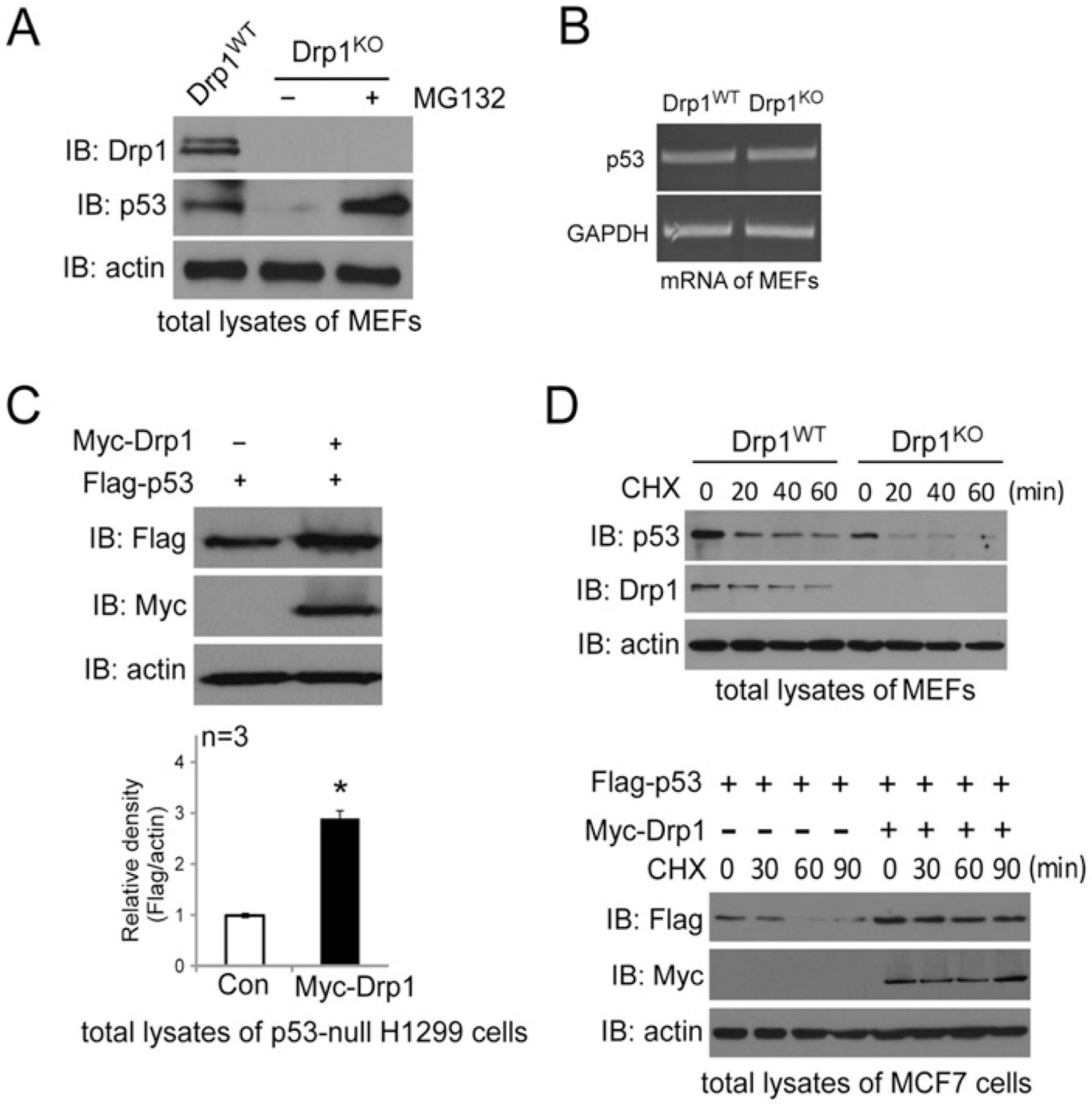

Figure 1. Drp1 stabilizes p53

(**A**) Drp1^{WT} or Drp1^{KO} MEFs were treated with the proteasome inhibitor MG132 (10 μM for 6 h). Total lysates were determined by Western blot analysis using anti-Drp1 or anti-p53 antibodies. Actin was used as a loading control. (**B**) Total RNA was extracted from Drp1^{WT} or Drp1^{KO} MEFs. The p53 mRNA level was determined by RT (reverse transcription)–PCR, and GAPDH (glyceraldehyde-3-phosphate dehydrogenase) was an internal control. The primers are listed in Supplementary Table S1 (http://www.biochemj.org/bj/461/bj4610137add.htm). (**C**) H1299 cells were transfected with a constant amount of FLAG–p53

together with Myc–Drp1 or control vector. Total protein levels of p53 and Drp1 were determined by Western blot analysis, and actin was a loading control. *P< 0.05 compared with control (Con). (**D**) Upper panel: cycloheximide (CHX)-chase experiments of p53 in $Drp1^{WT}$ or $Drp1^{KO}$ MEFs are shown. Lower panel: FLAG–p53 was co-transfected with Myc–Drp1 or control vector. The cells were treated with CHX at 50 μg/ml at the times indicated. The half-life of p53 was determined by Western blotting. Actin was used as a loading control. IB, immunoblot.

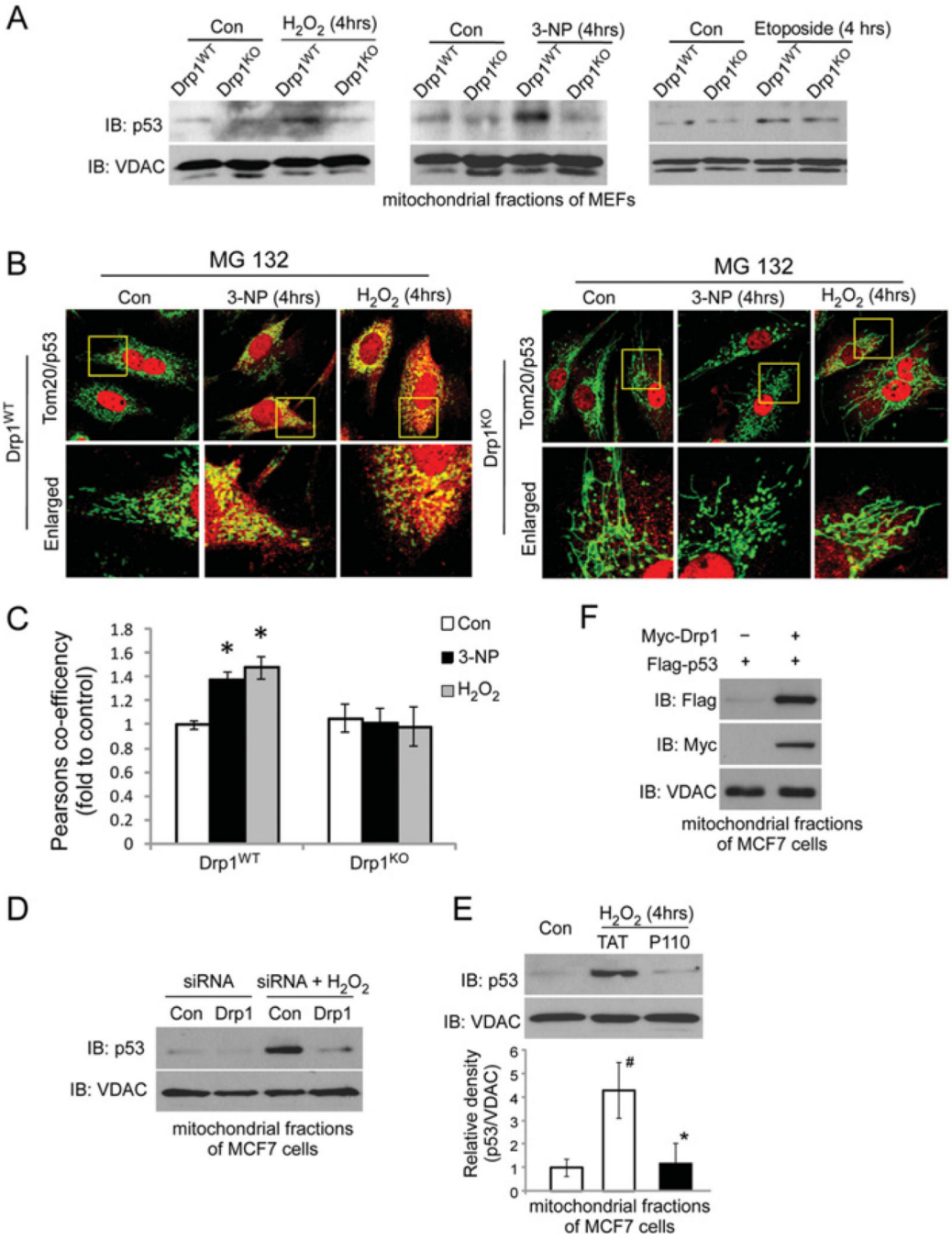

Figure 2. Drp1 is required for p53 translocation to the mitochondria under conditions of oxidative stress

(**A**) Drp1^{WT} or Drp1^{KO} MEFs were treated with H_2O_2 (600 μM, 4 h), 3-NP (10 mM, 4 h) or etoposide (100 μM, 4 h). Western blot analysis of mitochondrial fractions was carried out using anti-p53 antibodies. VDAC was used as a loading control. (**B**) Drp1^{WT} or Drp1^{KO} MEFs were treated with MG132 (3 μM for 4 h). Confocal imaging analysis was carried out using anti-p53 (1:2000 dilution, red) and anti-Tom20 (a marker of mitochondria, 1:500 dilution, green) antibodies. Lower panels provide enlargement of the boxed areas in the

upper panels. Scale bar, 5 μm. (**C**) p53/Tom20 co-localization in (**B**) was determined using a confocal microscopy programme (Pearson's co-efficient). Results are means ± S.D. for three independent experiments. At least 100 cells per group were counted. **P*< 0.05 compared with control cells. (**D**) MCF7 cells were transfected with control or Drp1 siRNA for 36 h. Cells were treated with H_2O_2 (600 μM) for 4 h. (**E**) MCF7 cells were incubated with P110 or control peptide Tat (1 μM, each) for 12 h before the addition of H_2O_2 (400 μM) for 4 h. (**F**) MCF7 cells were transfected with the indicated plasmids. Western blot analysis of mitochondrial fractions was carried out with anti-p53 antibodies. VDAC was used as a loading control. Quantification results are means ± S.D. for three independent experiments. $^{\#}P$< 0.05 compared with control cells; **P*< 0.05 compared with Tat-treated cells. Con, control; IB, immunoblot.

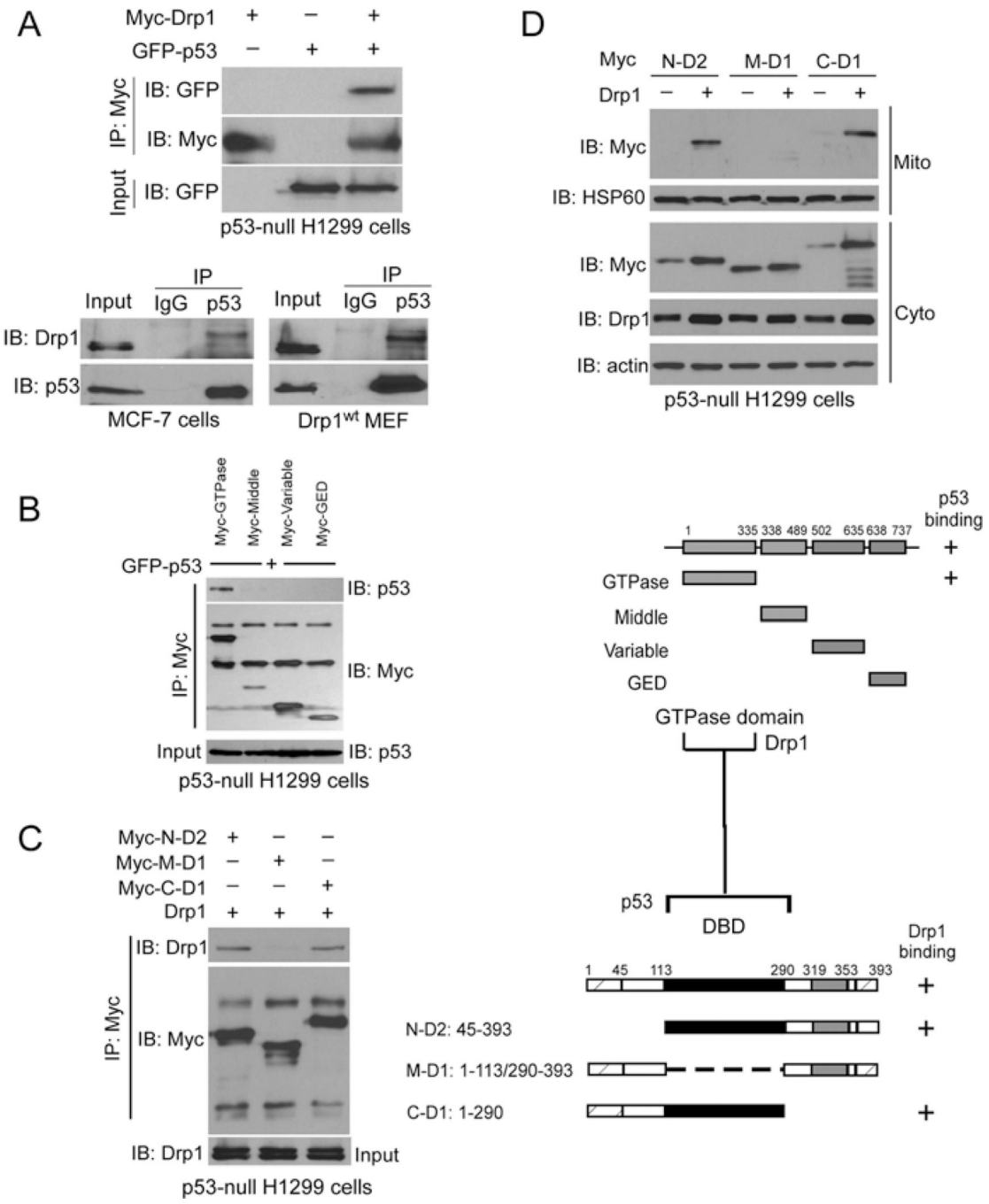

Figure 3. Drp1 binds to p53

(**A**) Upper panel: GFP–p53 was co-expressed with Myc–Drp1 in H1299 cells. Immunoprecipitates (IP) with anti-Myc were immunoblotted (IB) with anti-GFP antibody. Lower panel: immunoprecipitates with anti-p53 in Drp1^{WT} MEFs and MCF-7 cells were immunoblotted with the anti-p53 and anti-Drp1 antibodies. (**B**) Mapping analysis on the interaction between Drp1 and p53. Left: H1299 cells were expressed with the indicated Drp1 truncated mutants. Immunoprecipitates with anti-Myc antibody were determined by Western blot analysis using the indicated antibodies. Right: map of Drp1 truncated mutants.

The region that interacted with p53 is labelled ‘ + ‘. GED, GTPase-effector domain. (**C**) Left: H1299 cells were expressed with a series of p53 deletion mutants, and immunoprecipitates with anti-Myc antibodies were immunoblotted with the indicated antibodies. Right: map of p53 truncated mutants. The region that interacted with Drp1 is labelled ‘ + ‘. The data suggest that the GTPase domain of Drp1 interacts with the DBD of p53. (**D**) H1299 cells were transfected with the indicated plasmids. Western blot analysis of mitochondrial and cytosolic fractions was carried out with the indicated antibodies. HSP60 was used as a mitochondrial loading control, and actin was used as a cytosolic loading control. IB, immunoblot; IP, immunoprecipitation.

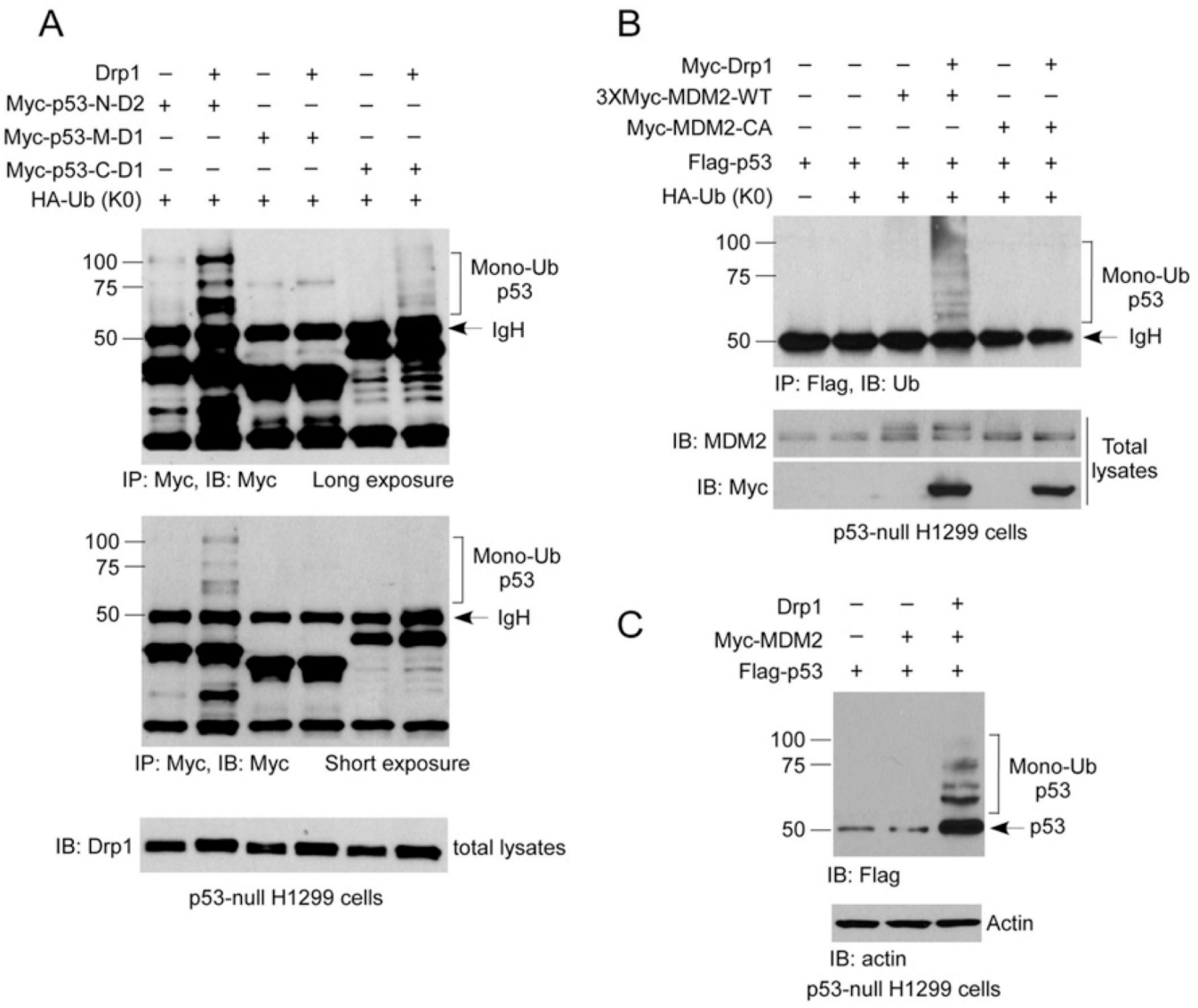

Figure 4. Drp1 induces p53 mono-ubiquitination

(**A**) H1299 cells were co-transfected with the indicated plasmids. Cells were treated with MG132 (10 μM) for 12 h, followed by immunoprecipitation with anti-Myc antibody, and then the ubiquitinated p53 was analysed. (**B**) H1299 cells were co-transfected with the indicated plasmids (see the text for details). The ubiquitination of p53 was analysed by Western blotting using an anti-FLAG antibody. Actin was used as a loading control. (**C**) H1299 cells were co-transfected with the indicated plasmids. Cells were treated with MG132 (10 μM) for 12 h. Ubiquitinated p53 was immunoprecipitated and detected with anti-ubiquitin (Ub) antibody. Mono-ubiquitinated p53 forms are indicated on the right. Sizes of molecular-mass markers are indicated on the left in kDa. IB, immunoblot; IP, immunoprecipitation.

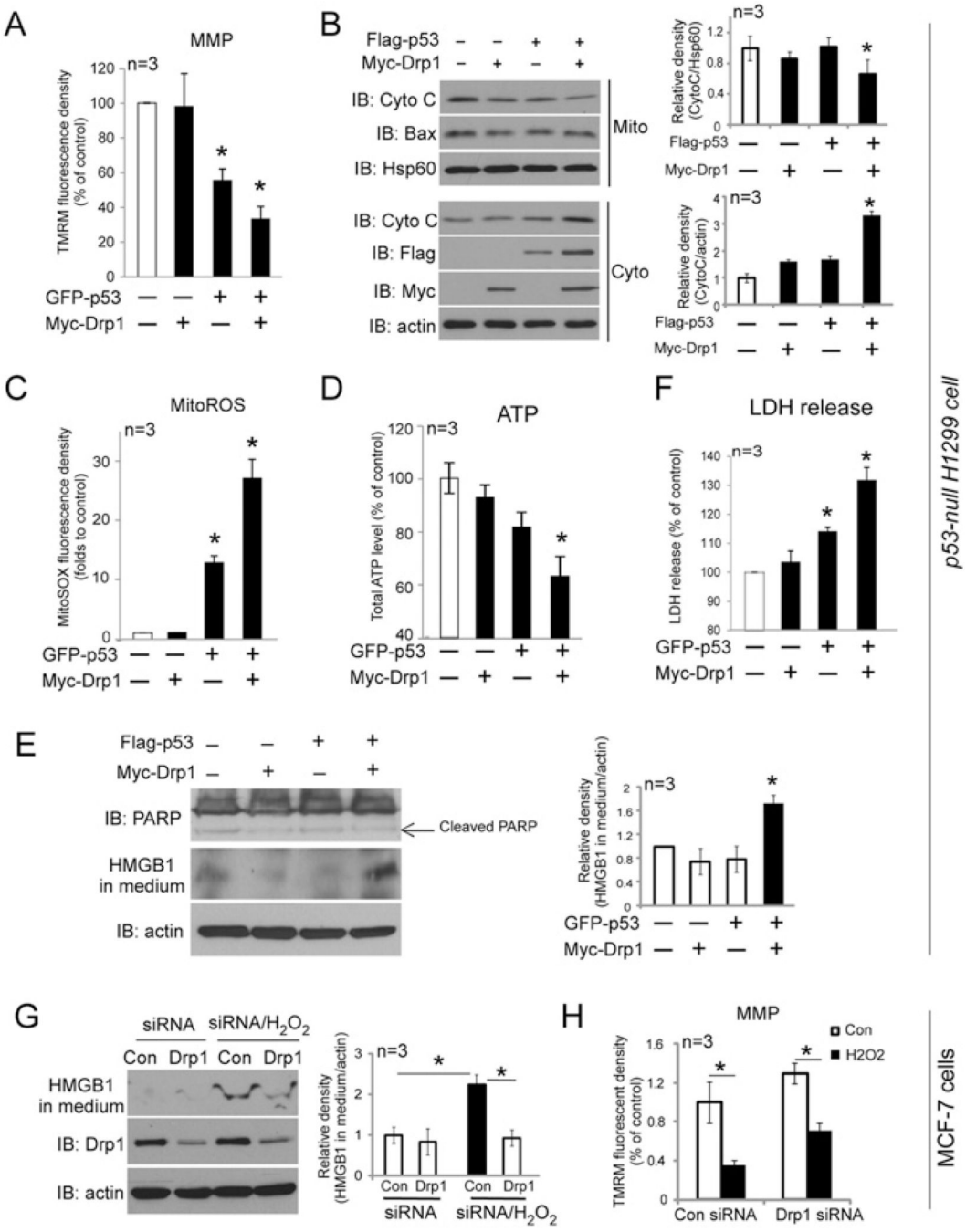

Figure 5. Drp1 and p53 interdependently induce mitochondrial damage and trigger necrosis

(**A, C, D** and **F**) p53-null H1299 cells were co-expressed with GFP–p53 and/or Myc–Drp1. MMP, mitoROS production, total ATP levels and LDH release were determined. **P*< 0.05 compared with control group. (**B**) H1299 cells were expressed with FLAG–p53 and/or Myc–Drp1. At 24 h after transfection, Bax and cytochrome *c* were examined in mitochondrial (Mito) and cytosolic (Cyto) fractions by immunoblotting. VDAC was used as a loading control for mitochondrial fractions. The protein levels of Bax and cytochrome *c*(Cyto C) were quantified. **P*< 0.05 compared with control group. (**E**) H1299 cells were expressed

with FLAG–p53 and/or Myc–Drp1. At 24 h after transfection, PARP cleavage and HMGB1 release were determined by immunoblotting. Actin was used as a loading control. The level of HMGB1 was quantified. **P*< 0.05 compared with control group. MCF7 cells were transfected with control or Drp1 siRNA. After 36 h of transfection, cells were treated with H_2O_2 (600 μM) for 12 h. (**G**) Quantification of HMGB1 release in medium. (**H**) MMP was determined. **P*< 0.05. Results in all histograms are means ± S.D. for three independent experiments. Con, control; IB, immunoblot.

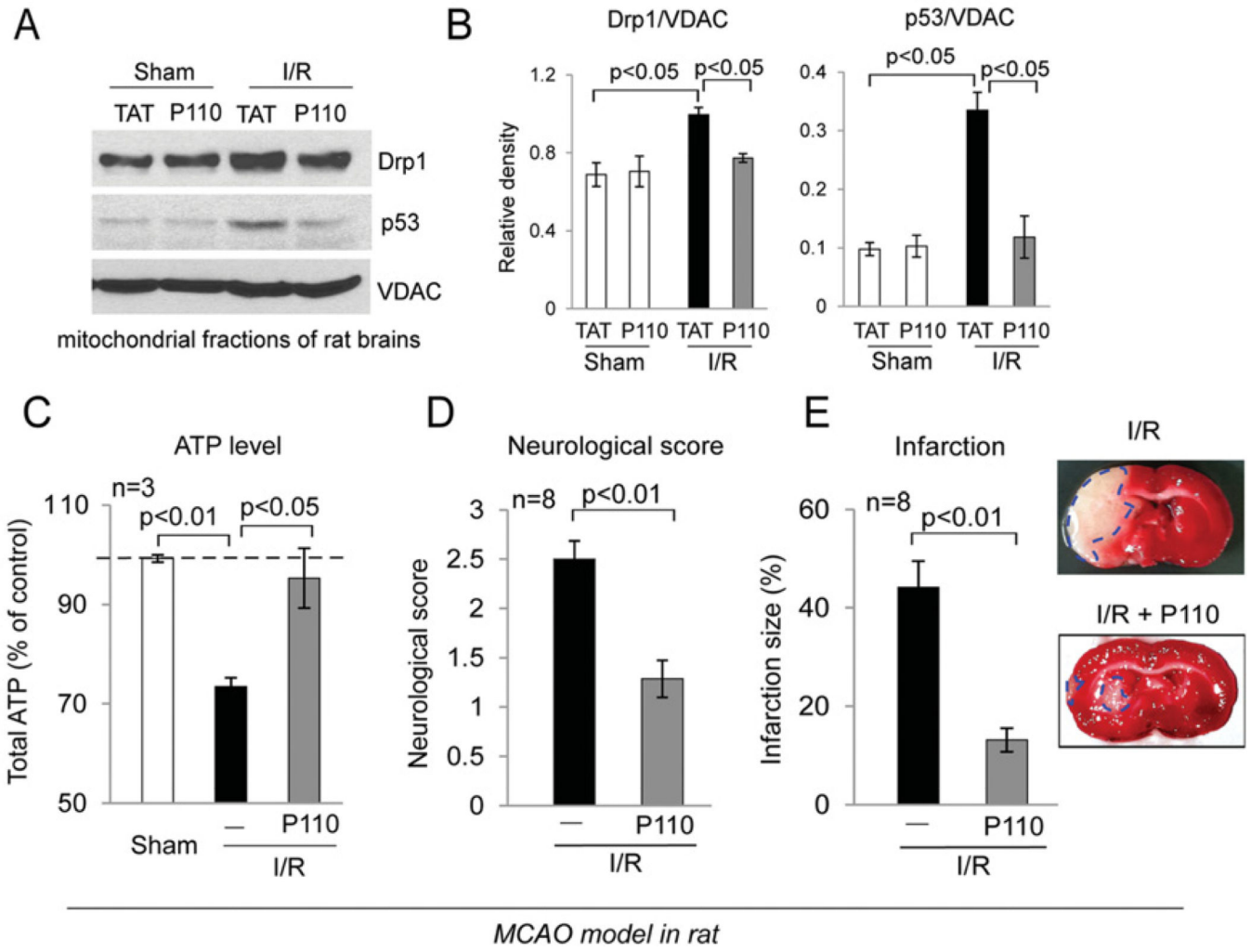

Figure 6. Inhibition of Drp1 hyperactivation suppresses p53 mitochondrial accumulation and reduces brain infarction in rats subjected to brain ischaemia/reperfusion

Rats were intraperitoneally injected with control peptide carrier Tat or Drp1 peptide inhibitor P110 (0.5 mg/kg of body weight) immediately before ischaemia. (**A**) Mitochondrial fractions were isolated from the striatum of rats subjected to 2 h of ischaemia followed by 2 h of reperfusion. Both Drp1 and p53 mitochondrial levels were determined by Western blot analysis. VDAC was used as a loading control. A blot representative of three rats is shown. (**B**) Quantification of Drp1 and p53 mitochondrial levels. (**C**) Total brain lysates were prepared after 2 h of ischaemia/24 h of reperfusion, and the ATP level was determined. (**D**) The neurological status of the rats after 24 h of reperfusion was evaluated by an observer blinded to the treatment groups. The score for each rat was recorded. (**E**) Infarction size (circled in blue) was determined by NIH ImageJ software. Results in all histograms are means ± S.D. for *n* experiments as indicated. I/R, ischaemia/reperfusion.